[19]Model No. 144 with capsule type 1, Texas Instruments, Inc., Houston, Tex.
[20]W. H. Keesom, *Helium* (Elsevier, Amsterdam, 1942).
[21]R. E. Barieau, J. Phys. Chem. 72, 4079 (1968).
[22]S. G. Sydoriak and T. R. Roberts, Phys. Rev. 118, 901 (1960).
[23]T. R. Roberts and B. K. Swartz, in *Proceedings of the Second Symposium on Liquid and Solid Helium Three*, edited by J. G. Daunt (Ohio State U. P., Columbus, Ohio 1960).
[24]R. de Bruyn Ouboter, J.J. M. Beenakker, and K. W. Taconis, Physica 25, 1162 (1959).
[25]T. R. Roberts and S. G. Sydoriak, Phys. Fluids 3, 895 (1960).
[26]M. J. Buckingham and W. M. Fairbank, in *Progress in Low Temperature Physics*, edited by C. J. Gorter (North-Holland, Amsterdam, 1961), Vol. III, Chap. 3.
[27]Complete tables of the values of $c_{P,x}$ so determined may be obtained from the last author (W. Z.).
[28]Reference 4, Fig. 12. Note that these measurements were made with a full cell and at a pressure that was probably somewhat above saturated vapor pressure. Therefore, the specific heat measured was not strictly the same as our c, although the difference is likely to have been quite small.
[29]R. Radebaugh, Nat. Bur. Std. (U.S.) Technical Note No. 362, 1967 (unpublished).
[30]D. O. Edwards and J. G. Daunt, Phys. Rev. 124, 640 (1961).
[31]In making the plots of Fig. 9 from the tabulated data for $c_{P,x}$, shifts in T_λ of up to 1.0 m°K between the separate series of points involved were allowed in order to bring the data of these series into better agreement.
[32]M. E. Fisher and P. E. Scesney, Phys. Rev. A 2, 825 (1970).
[33]F. London, *Superfluids* (Wiley, New York, 1954), Vol. II, Sec. 7.
[34]*Collected Papers of L. D. Landau*, edited by D. ter Haar (Pergamon Press, Oxford, 1965), p. 193.
[35]G. Ahlers, Phys. Rev. 171, 275 (1968).
[36]R. W. Hill and O. V. Lounasmaa, Phil Mag. 2, 143 (1957).

PHYSICAL REVIEW A VOLUME 4, NUMBER 6 DECEMBER 1971

Validity of the Quasisteady State and Collisional-Radiative Recombination for Helium Plasmas. I. Pure Afterglows*

C. C. Limbaugh†
Arnold Engineering Development Center, Arnold Air Force Station, Tennessee

and

A. A. Mason‡
The University of Tennessee Space Institute, Tullahoma, Tennessee

(Received 6 February 1971)

The set of differential equations describing the time-dependent decay of a singly ionized optically thin monatomic gas has been solved numerically for constant-temperature–constant-pressure helium afterglows. In the range of conditions studied ($6000 \leq T_e \leq 14\,000$ °K, $1.5\times10^{12} \leq n_e \leq 5.38\times10^{15}$ cm^{-3}, $1.5\times10^{14} \leq n_0 \leq 1.63\times10^{17}$ cm^{-3}) it was found that collisional-radiative recombination can be applied to the electron-density decay before the plasma reaches the quasisteady state. The initial condition for each plasma studied was a Boltzmann distribution from the $2\,^3S$ state throughout the higher states. The mechanism by which the quasisteady state is obtained is examined and the transient coupling between states is illustrated. Times for the plasma to reach the quasisteady state ranged from $t \approx 10^{-8}$ sec for high-density plasmas to $t \approx 10^{-4}$ sec for low-density plasmas.

I. INTRODUCTION

The study of recombining plasmas was considerably enhanced by the development of the collisional-radiative recombination (CRR) theory by Bates, Kingston, and McWhirter[1] for hydrogenic plasmas. Their work included three-body recombination[2] along with the other salient processes contributing to plasma decay to obtain effective collisional-radiative recombination and collisional-radiative ionization coefficients which describe the plasma decay. In order to obtain their results, however, it is necessary to impose the quasisteady state (QSS) assumption in which all quantum levels, with the exception of the ground state, do not suffer a temporal change in population density. Another approach[3,4] to obtaining CRR coefficients utilizing the fact that there is a minimum in the total rate of deexcitation of atoms as a function of the energy levels has been used but this also requires the QSS assumption.

The results of CRR theory and the QSS assumption have been used by many investigators (e.g., Refs. 5–8) to interpret results for helium plasmas with varying degrees of success. Although in much of the work the existence of the molecular

helium ion was suspected as being responsible for diverse results,[9] most of the helium work appears to compare experimentally measured recombination coefficients directly with the hydrogen calculations of Ref. 1. Chen[10] calculated CRR coefficients, α, for helium and found them generally to lie below the hydrogenic coefficients at the same plasma conditions. The same work obtained experimental values of α in fairly good agreement with calculations.

A common factor in all experimental determinations is that the plasma is not quiescent but rather is itself in a transient condition. If the transients are sufficiently rapid that the plasma cannot be viewed as progressing from one QSS to the next, with the population densities adjusting themselves to the QSS distribution at the current conditions "almost instantaneously," then a basic assumption of CRR is violated and the applicability is in serious jeopardy. There have been timing studies to determine decay time for some specific energy level to return to QSS[11,12] following a plasma perturbation but these also depended upon the rest of the plasma maintaining its QSS distribution and did not take into account the transient coupling between states. This transient coupling between states makes it difficult to assess confidently the time for the QSS to be achieved or to determine the transient effects upon measured recombination rates. Indeed, it is this transient coupling which describes the mechanisms by which the QSS is established and this cannot be studied without removing the QSS assumption.

To study this transient coupling between the energy states and to study the detailed process by which the QSS is established so as to evaluate critically the applicability of CRR theory, the transient solution to the eigenstate rate equations (ERE) for helium has been made. (The distinction between the ERE and CRR is made because CRR mathematically implies the QSS assumption, which is explicitly removed in this study. As will be seen, the CRR process can apply physically independent of the QSS for description of the electron density.) Earlier work on the ERE for hydrogen[13] investigated the fundamental consistency of the solution to the ERE and convergence to the CRR. The work has been extended to helium because of a wider range of experimental data available in the literature. Somewhat more care has been exercised to preserve certain aspects of the solution so that details of the acquisition of the QSS can be observed. Other work[14] examined the solution to the ERE for hydrogen with the plasma being subjected to sudden severe changes in plasma parameters such as excitation temperature or free-electron density. It was shown that these parametric changes can have an appreciable effect upon the plasma decay. Although detailed quantitative comparisons between the results of Refs. 13 and 14 are difficult because of the different problems being solved (Ref. 13 was concerned with the afterglow problem), they do show qualitative agreement with each other and other unpublished work by the present authors. The work in this paper appears to be the first published in which the characteristics of the ERE are applied to helium.

II. THEORY

The basic set of equations from which the CRR model is derived has been developed elsewhere[1] and will not be repeated here. The result of the development is an infinite system of nonlinear coupled differential equations describing the time rate of change of the population density of each energy state available to the plasma. Each equation is of the form

$$\frac{dn(p)}{dt} = -n_e n(p) K(p; c) - n_e n(p) \sum_q K(p; q) - n(p) \sum_{q<p} A(p; q) + n_e \sum_q n(q) K(q; p) + \sum_{q>p} n(q) A(q; p) + n_e^2 \beta(p) + n_e^2 K(c; p) , \quad (1)$$

where p and q symbolically represent energy states available to the bound electron, n is the population density, and the subscript e denotes the free-electron continuum. The $K(p; c)$ and $K(c; p)$ are rate coefficients for electron collisional ionization of the p state and three-body collisional filling of the p state, respectively. $K(p; q)$ and $K(q; p)$ are rate coefficients for electron collisional excitation or deexcitation resulting in depopulating state p to any other state q or populating state p from any other state q, respectively. $A(p; q)$ is the Einstein spontaneous transition probability for radiative transitions from state p to state q and in the formulation of Eq. (1) may be zero if the dipole selection rules are violated. $\beta(p)$ is the radiative recombination rate coefficient for filling state p.

Thus, in Eq. (1), the first term expresses the rate of depopulation of state p because of electron-atom ionizing collisions. The second term is the rate of depopulation of state p because of electron-atom inelastic collisions changing the bound electron to a higher state ($p < q$) or electron-atom superelastic collisions in which the bound electron goes to a lower-energy state ($p > q$). The third term represents the rate of depopulation of state p because of radiative transitions from state p to a lower state q. The last four terms represent the rate of population of state p because of electron-atom inelastic collisions, radiative transitions from some higher state q, radiative recombination, and three-body recombination, respectively.

Equation (1) as written represents an infinte

rectangular system describing the complete temporal behavior of the population density distribution for a singly ionized optically thin monatomic plasma in which there are no spatial gradients nor heavy body collisions. By adding the equation for conservation of particles

$$\sum_p n(p) + n_e = n_0 , \tag{2}$$

where n_0 is the total number density, the system becomes square and, in principal, determinate.

Additionally, in this work the electron temperature will be assumed constant at a value somewhat above the quasiequilibrium temperature indicated by Bates and Kingston.[15] This assumption does not consider the effect of radiative losses, elastic electron-heavy body collisions, and possible wall effects upon the electron temperature. This simplification is admittedly at variance with observed physical behavior in that a decaying electron temperature has been observed in virtually every afterglow experiment. However, inclusion of a time-dependent electron temperature greatly increases the complexity of the problem by requiring instantaneous evaluation of the rate coefficients without contributing to the elucidation of the mechanisms by which the QSS distribution is established. In the transient situation a decaying electron temperature has the effect of reducing the collisional rate coefficients and thus increasing the importance of radiation. Qualitatively this does not affect the present model because the initial density distribution was chosen such that the direction of change of the individual state densities in approaching the final QSS distribution is determined by radiative effects. This is true even though the state may be strongly collision dominated because, in a Boltzmann configuration, collisional processes contributing to the populating and depopulating of a specific level effectively cancel, leaving the radiation terms as the determining factors. Thus, with the assumption of a constant electron temperature, the present study is believed to model qualitatively the physical processes by which the QSS is approached, even in an environment in which the electron temperature decays.

The rate coefficients for ionization $[K(p; c)]$ and excitation $[K(p; q),\ p < q]$ were evaluated by integrating the Gryzinski formulation[16] of the energy-dependent cross section for the transition over a Maxwellian energy distribution for the free electrons. The evaluation of the excitation rate coefficients $K(p; q)$ included both direct excitation (satisfying dipole selection rules) and exchange excitation (loosely defined as not satisfying the dipole selection rules). The Gryzinski formulation for each of these processes refers to a transfer of energy from the projectile electron to the bound electron that is just sufficient to excite the bound electron to the desired state. When the projectile electron has more than enough kinetic energy to effect this transition, the probability of excitation to the next higher state must be subtracted or

$$Q(p; q) = Q(E_e, E_{p,q}) - \sum_{i=0}^{I} Q(E_e, E_{p,q+i}),$$

$$E_{p,q+I} \le E_{p,q+I+1} \tag{3}$$

where $Q(p; q)$ is the cross section for the reaction and $Q(E_e, E_{p,q+i})$ refers to the functional dependence of Q upon the electronic kinetic energy E_e and the energy necessary to elevate a bound electron from its orbit E_p to some higher orbit E_{q+i}. The rate coefficients for three-body recombination $[K(c; p)]$ and superelastic collisions $[K(p; q),\ q < p]$ were obtained from the rate coefficients for electron-atom inelastic collisional ionization and excitation, respectively, using the principal of detailed balance. Spontaneous transition probabilities were taken from Niles[17] who covered the most important transitions to the lower levels. Transitions among the upper levels were included by using the hydrogen approximation and the radial matrix elements of Green, Rush, and Chandler.[18] Helium energy levels were taken from Moore.[19] Seaton's expression for hydrogen radiative recombination[20] was modified for helium energies and multiplicities.

The system of equations symbolized by Eqs. (1) and (2) can be truncated at a finite quantum level by noting that there will be some quantum level above which all population densities are in equilibrium with the free electrons.[1,5] This is the so-called critical level[5] and its existence means that those states above it have their temporal characteristics described fully by the temporal characteristics of the continuum. It is not necessary to include more than a few states above this critical level because the relative importance of reactions causing a transfer of a bound electron to another bound state across the critical level falls off rapidly with increasing energy difference.

For this study singlet and triplet states were maintained separate through quantum level 6. All substates were summed together for each of the levels 7–10. Core size on the available computer dictated that the system not be allowed much larger so no higher quantum levels were kept distinct. However, to provide a reservoir for processes affecting the high quantum levels (7–10), levels 11–15 were summed together and included as one state. Thus the study is restricted to conditions such that at least quantum level 10 is in equilibrium with the free electrons.

It is at this point that previous investigators imposed the QSS assumption.[1] Under this assumption, the time rates of change of all excited states are

assumed negligibly small compared to the rate of change of the ground state and continuum. Hence, at QSS, $\dot{n}(1) = -\dot{n}_e$. As a consequence of this the time rate of change of either the ground state or the free-electron density is described by an effective three-body recombination coefficient called the collisional-radiative recombination coefficient or, at QSS,

$$\dot{n}(1) = -\dot{n}_e = \alpha n_e^2 , \tag{4}$$

where α is the CRR coefficient. It should be noted that this nomenclature is different than the original work of Ref. 1 where the coefficient identified as the CRR coefficient in Eq. (4) is termed the collisional-radiative decay coefficient. The CRR coefficient in Ref. 1 was identified and paired with the collisional-radiative ionization coefficient such that

$$\gamma = \alpha_{\mathrm{CRR}} - S n(1)/n_e , \tag{5}$$

where S is the collisional-radiative ionization coefficient. γ is the collisional-radiative decay coefficient of Ref. 1 and is to be identified with α in Eq. (4). For most applications of interest, the second term in Eq. (5) is negligible and common usage has developed the nomenclature that α defined in Eq. (4) is identified as the CRR coefficient. This terminology is adhered to in this paper.

Although QSS is certainly a reasonable assumption and results from the CRR theory have enjoyed success, the QSS assumption by its very nature prevents a study of the time and mechanism whereby the QSS is actually obtained.

This study has undertaken the transient solution to the ERE for helium without implementing the QSS assumptions by applying numerical techniques directly to the system of equations represented by Eqs. (1) and (2). The technique used in this study is the implicit modified Euler's method[21] and differs from the earlier work[13] which used a Taylor series expansion to obtain the solution. The use of the present method is a significant improvement over the method of Ref. 13 in that computer run times are considerably shortened: Average run time for the data presented here is about 1 h for each condition studied on an IBM S360/50 computer using the IBM H-level Fortran compiler to fully optimize the machine code. Gordiets, Gudsenko, and Shelepsin[14] used the Runge-Kutta method to integrate the rate equations but no comparative run times are available.

The earlier work[13] established the fundamental validity of the ERE and of the transient solution they will produce. The present work, carried out on helium, investigates the actual details of the acquisition of the QSS for several plasmas. By examining the transient solution including the coupling between the various states and the time for QSS to be reached, insight into the validity of CRR to experimental plasmas will be obtained.

III. RESULTS

The transient solutions to the ERE under the restrictions and assumptions previously indicated were obtained for the plasma conditions summarized in Table I. The lower limits of electron temperature, ionizations, or total number density represent approximate lower bounds to the plasmas which could be solved with the present computer program because of the critical level limits described earlier. Although conditions above the upper limits of the parameters have not been investigated it is believed that extension will not yield notably different data on the mechanism by which QSS is established. The initial distribution for each of these cases was chosen to be a Boltzmann configuration for all excited states.

Much of the data to be presented here will be examination of instantaneous rates of decay for the various quantities. Rates are much more sensitive than the population densities and provide a more critical examination of the QSS.

A. QSS Recombination Coefficients

For comparative purposes, the QSS collisional-radiative recombination coefficients, α, were obtained for those plasmas studied and the results are shown in Table II together with results interpolated from those reported by Chen.[10]

The present results are obtained by allowing the transient solution to develop until $\dot{n}_e$ and $\dot{n}(1)$ agree to within 5% and then calculating α with the instantaneous values of $\dot{n}_e$ and n_e^2, $\alpha = -\dot{n}_e/n_e^2$.

As is seen, the present results from the ERE compare favorably with those of Chen, being consistently slightly lower except for the low-temperature case D. Chen also used Gryzinski's technique for obtaining collision cross sections but used a different source for the radiative transition probabilities. Chen did not include all collisional transitions as this work does and Chen used the simplified technique of obtaining the minimum in the total

TABLE I. Summary of plasma conditions studied with ERE.

Case	n_0 (cm^{-3})	n_e/n_0	T_e (°K)
A	1.63×10^{17}	0.01	1.0×10^4
B	1.5×10^{16}	0.01	1.0×10^4
C	1.5×10^{14}	0.01	1.0×10^4
D	1.5×10^{16}	0.01	6.0×10^3
E	1.5×10^{16}	0.01	1.4×10^4
F	2.69×10^{15}	0.2	1.0×10^4
G	2.69×10^{15}	0.01	1.0×10^4
H	2.69×10^{15}	0.001	1.0×10^4

rate of deexcitation as a function of the energy levels of excited states.[3,4] These differences can easily account for the slight differences in Table II. It is believed that the inconsistent behavior of case D is due to the explicit inclusion of exchange excitations from the metastable 2^3S level to the adjacent metastable 2^1S level. This has the effect of maintaining a higher collisional rate to the nearby 2^1P level (rapid direct excitation) so that a higher rate of radiation to the ground state is maintained. This rate at QSS is communicated back through the bound states to the free electrons, thus resulting in a higher rate of recombination. Others[22] have also calculated recombination coefficients but their conditions and resolution of their data make comparisons difficult.

It is notable that these recombination coefficients are typically a factor of 2 below those reported for hydrogen by Bates *et al.*[1] This corresponds to a general trend in reported experimental values for helium recombination rates to be below hydrogen recombination rates (e.g., Refs. 6, 8, 23, and 24). The true value will be somewhat in doubt because of the inability of the Gryzinski cross sections to predict accurately the true collision rates. However, use of a consistent set of cross sections for both hydrogen and helium will indicate relative differences. The factor of 2 corresponds to the difference in the statistical weight of the ground-state ions of hydrogen and helium and the subsequent effect upon three-body recombination rate coefficients through the modified Saha equation.

B. Location of Critical Level

The initial distribution for each of the plasmas was an equilibrium distribution from the 2^3S level through the upper states considered. As the ERE solution develops in time, the levels below some critical level, defined to be that lowest quantum level which is maintained in equilibrium with the free electrons, adjust to the final QSS distribution while those levels above and including the critical level remain in equilibrium with the free electrons.

TABLE II. Quasisteady state collisional-radiative recombination coefficients from ERE solution.

Case	T_e (°K)	n_e (cm^{-3})	α(ERE) (cm^3/sec)	α [a] (cm^3/sec)
A	1.0×10^4	1.63×10^{15}	5.9×10^{-12}	7.0×10^{-12}
B	1.0×10^4	1.5×10^{14}	2.16×10^{-12}	2.25×10^{-12}
C	1.0×10^4	1.5×10^{12}	6.77×10^{-13}	8.1×10^{-13}
D	6.0×10^3	1.5×10^{14}	1.25×10^{-11}	8.5×10^{-12}
E	1.4×10^4	1.5×10^{14}	7.98×10^{-13}	1.05×10^{-12}
F	1.0×10^4	5.38×10^{14}	3.32×10^{-12}	3.7×10^{-12}
G	1.0×10^4	2.69×10^{13}	1.26×10^{-12}	7.35×10^{-12}
H	1.0×10^4	2.69×10^{12}	6.86×10^{-13}	8.5×10^{-13}

[a]Reference 10.

TABLE III. Total number density, electron density, electron temperature, and location of critical level for each of the plasmas studied.

Case	n_0 (cm^{-3})	n_e (cm^{-3})	T_e (°K)	Critical level (principal quantum number) 3%	10%
A	1.63×10^{17}	1.63×10^{15}	1.0×10^4	4	4
B	1.5×10^{16}	1.5×10^{14}	1.0×10^4	5	4
C	1.5×10^{14}	1.5×10^{12}	1.0×10^4	9	7
D	1.5×10^{16}	1.5×10^{14}	6.0×10^3	6	5
E	1.5×10^{16}	1.5×10^{14}	1.4×10^4	5	4
F	2.69×10^{15}	5.38×10^{14}	1.0×10^4	5	4
G	2.69×10^{15}	2.69×10^{13}	1.0×10^4	6	5
H	2.69×10^{15}	2.69×10^{12}	1.0×10^4	8	6

Although the present computations are not based on a concept of a critical level, the observation of its development in the transient solution and its location is of interest pertaining to the internal consistency of the calculations. The location of the critical level is useful for experimental determinations because it indicates that lowest level whereby spectral intensity measurements can be used to ascertain the kinetic temperature of the free-electron distribution.

Table III lists the critical levels found for each of the plasmas as well as the total density, electron density, and electron temperature. Two criteria were used for identification of the critical level: 3 and 10% referring to the maximum deviation from equilibrium with the free electrons for any of the substates for the principal quantum level to be considered as the critical level.

The critical levels found for the high-electron density high-temperature cases with the 10% criteria compare favorably with predictions by Hinnov and Hirschberg,[5] who indicate that at those conditions, quantum number 4 will be the lowest level in equilibrium with the free electrons. No comparisons were made at the low densities and temperature other than to observe that they qualitatively show expected behavior.

C. Time Development of ERE Solution

The time development of the QSS for each of the plasmas as a whole is illustrated in Figs. 1–3. Two curves are plotted for each case. One, the ratio of the continuum rate to the ground-state rate $\dot{n}_e/\dot{n}(1)$ has the value -1 at QSS. The other, the ratio of the time-dependent CRR coefficient, $\alpha(t) = -\dot{n}_e/n_e^2$, to the value of α at QSS, has the value $+1$ at QSS or when CRR theory will describe the continuum decay.

A consequence of the QSS for the optically thin plasma[1] is the condition that the rate of change of the ground-state density and the continuum density are equal in magnitude but opposite in sign. Hence, observation of the time development of the ratio

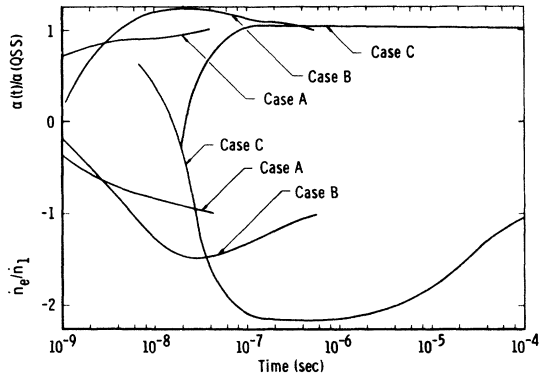

FIG. 1. Ratio of time rate of change of free-electron density to time rate of change of ground-state density and ratio of time-dependent collisional-radiative recombination coefficient to its value at QSS. $T_e = 10\,000\,°K$; 1% ionization; case A: $n_0 = 1.63 \times 10^{17}$ cm^{-3}; case B: $n_0 = 1.5 \times 10^{16}$ cm^{-3}; case C: $n_0 = 1.5 \times 10^{14}$ cm^{-3}.

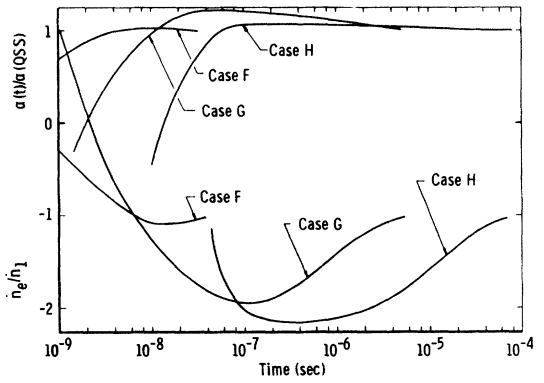

FIG. 3. Ratio of time rate of change of free-electron density to the time rate of change of ground-state density and ratio of time-dependent collisional-radiative recombination coefficient to its value at QSS as functions of time for various electron densities. $T_e = 10\,000\,°K$; $n_0 = 2.69 \times 10^{15}$ cm^{-3}; case F: $n_e = 5.38 \times 10^{14}$ cm^{-3}; case G: $n_e = 2.69 \times 10^{13}$ cm^{-3}; case H: $n_e = 2.69 \times 10^{12}$ cm^{-3}.

$\dot{n}_e/\dot{n}(1)$ will provide graphic illustration of the region in which the QSS is valid. Since the CRR coefficient used in this work is based totally upon the free-electron-density characteristics, examination of the time development of the CRR coefficient based upon instantaneous values of n_e and $\dot{n}_e$ and compared to the QSS will show the region in which CRR theory will be valid for application to electron-density measurements, irrespective of QSS conditions.

Figure 1 shows the effect of varying total number density and election density together. Figure 2 shows the effect of varying electron temperature. Figure 3 shows the effect of varying the electron density. As one would expect, as conditions are varied to lower collision rates, the time required for the QSS to be established is lengthened and becomes significant for low-density cases.

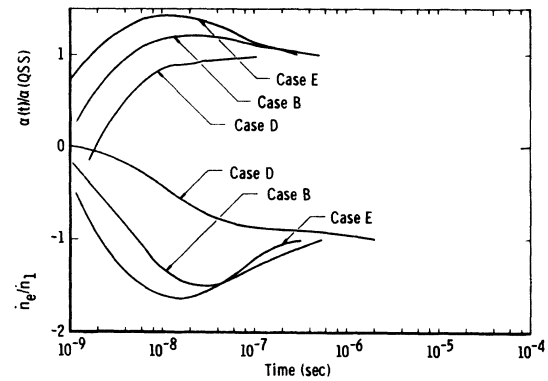

FIG. 2. Ratio of time rate of change of free-electron density to time rate of change of ground-state density and ratio of time-dependent collisional-radiative recombination coefficient to its value at QSS as functions of time for various temperatures. $n_0 = 1.5 \times 10^{16}$ cm^{-3}; $n_e = 1.5 \times 10^{14}$ cm^{-3}; case D: $T_e = 6\,000\,°K$; case B: $T_e = 10\,000\,°K$; case E: $T_e = 14\,000\,°K$.

Examining the $\dot{n}_e/\dot{n}(1)$ curves one sees that a consistent character of the decay of these plasmas is the apparent overshoot of the QSS early in the decay of most of the plasmas (cases A and D the only exceptions) and then the slow recovery back to the QSS. This could be due to an overshoot of QSS conditions of either $\dot{n}_e$ or $\dot{n}(1)$ but in fact both quantities show the character to a greater or lesser degree. It is also tempting to ascribe the overshoot to numerical inaccuracies in the program but as will be seen below it is in fact a physical phenomenon.

Figure 4 shows the detailed time development of the rates of change of the continuum as well as the $1\,^1S$, $2\,^3S$, and $2\,^3P$ bound states for case B, which is typical of the phenomena. Both the ground-state and free-electron rates overshoot their QSS values and converge back toward their QSS value slowly. Of specific interest in this context is the $2\,^3P$ level. By comparing the shape of the curves for the time development of the $2\,^3P$ and continuum rates, it is seen that the continuum overshoot follows the sudden growth of the $2\,^3P$ rate from about 5×10^{-9} sec through about 3×10^{-7} sec and then slowly falls to the QSS value with the fall of the $2\,^3S$ and $2\,^3P$ levels to the QSS. The early part of the continuum rate curve, $t \leq 10^{-9}$ sec, follows the adjustment of the other quantum levels towards their QSS values.

Figure 5 examines the time development of the $2\,^3P$ rate in somewhat more detail illustrating both the collisional and radiative contributions to the net rate. The radiative rate is initially posi-

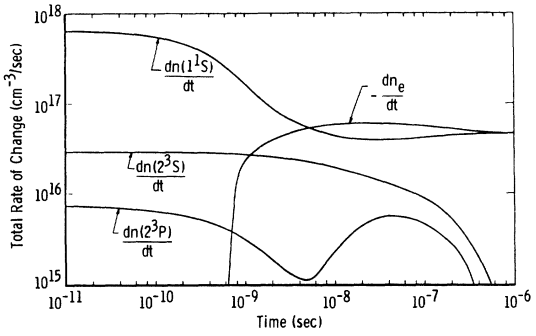

FIG. 4. Total rate of change of 1^1S, 2^3S, 2^3P quantum states, and free-electron density, case B. $T_e = 10\,000\,°K$; $n_0 = 1.5\times10^{16}$ cm^{-3}; $n_e = 1.5\times10^{14}$ cm^{-3}.

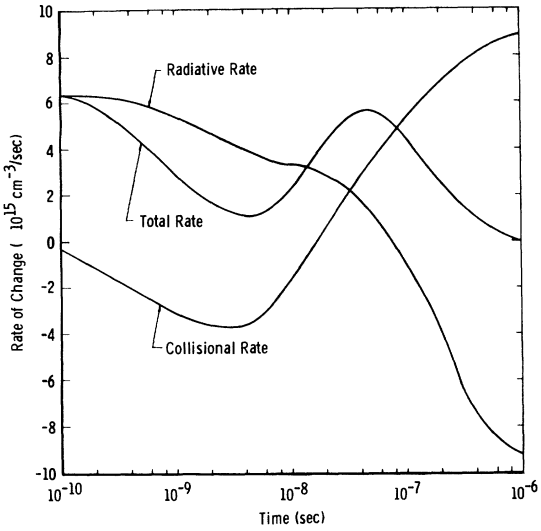

FIG. 5. Time development of total collisional rate, total radiative rate, and total rate of change of 2^3P state, case B. $T_e = 10\,000\,°K$; $n_0 = 1.5\times10^{16}$ cm^{-3}; $n_e = 1.5\times10^{14}$ cm^{-3}.

tive, the collisional rate negative, and thus the state is populating radiatively and depopulating collisionally with the radiative rate dominating. As the level continues to populate radiatively, the radiative depopulation rate to the 2^3S level becomes continually larger so the net radiative rate decreases toward zero at about 10^{-7} sec. Meanwhile the collisional depopulation rate also becomes larger with the increase in 2^3P density till about 4×10^{-9} sec. At this point the 2^3S level has become sufficiently populous that collisional transfers to the 2^3P level cause the 2^3P collisional depopulation rate to go through its maximum and begin decreasing. It is at this point that the total rate goes through its first minimum. Subsequent to 4×10^{-9} sec the 2^3S level continues to increase in density so that the 2^3P collisional rate continues to drive positive and at about 2×10^{-8} sec the collisional rate changes from a depopulating to a populating effect. The period 2×10^{-8} sec $\leq t \leq 10^{-7}$ sec is characterized by positive contributions to the total rate by both the collisional and radiative rates. The total rate goes through a maximum and decreases with the declining radiative rate. After about 10^{-7} sec the 2^3P level has become high enough in density that the radiative rate is dominated by radiative depopulation. The collisional population rate dominates the total rate, however, till about 10^{-6} sec when the 2^3S level is approaching QSS so the 2^3P radiative depopulation rate becomes large enough to balance the collisional population rate, and the total rate thus decreases to zero at QSS.

Figure 6 illustrates the time development of the population densities of the 2^3S, 2^3P, 2^1S, and 2^1P levels for case B. This shows the slow increase of the triplet states to their QSS value while examination of the singlet states reveals the cause of the ground-state rate overshoot shown in Fig. 4. The 2^1P level has a large radiative transition probability to the ground state. Hence its population density shows a very rapid decrease through the early part of the decay. As its density falls below the equilibrium configuration, collisions have a tendency to fill it and in particular collisional transfers from the 2^1S state. Hence the 2^1S state also shows a reduction in density but slightly lagging the 2^1P level. At about 1×10^{-8} sec, the 2^1P level has lowered in density sufficiently that collisional rates can begin to balance radiative rates so the density curve begins to flatten. However, the triplet states are continuing to increase in density so that exchange transfers between the triplet and singlet states become more numerous and serve to elevate the population densities of the singlet states. The largest single contributor to the ground-state rate is the radiative transitions from the 2^1P state. By comparing the ground-state rate in Fig. 4 to the 2^1P population density in Fig. 6 one sees that as the 2^1P density decreases, goes through a minimum,

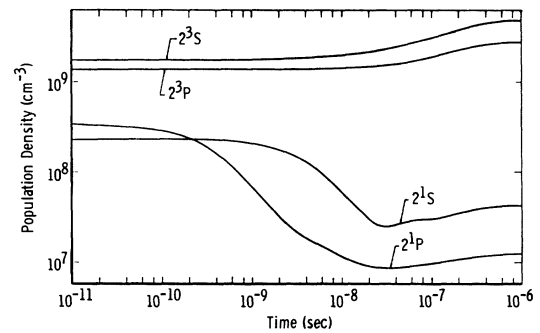

FIG. 6. Time development of population densities of 2^3S, 2^3P, 2^1S, and 2^1P states for case B. $T_e = 10\,000\,°K$; $n_0 = 1.5\times10^{16}$ cm^{-3}; $n_e = 1.5\times10^{14}$ cm^{-3}.

and slightly increases, so does the ground-state rate. The plasmas which show the overshoot in Figs. 1, 2, and 3 all exhibit this general behavior in the continuum and ground-state rates although the oscillation of the $2\,^3P$ rate is not present in the high-temperature case E.

Case E, which also shows the overshoot in both the ground-state and continuum rates is slightly more collision dominated at the low quantum levels in the early part of the decay. Thus collisions have a relatively more important role so that collisional transfers between the $2\,^3S$ and $2\,^3P$ levels occur with sufficient rapidity that the $2\,^3P$ rate does not show the oscillation prevalent in the lower-temperature plasmas. In this case, however, the singlet states still show the oscillation. This is because exchange collisions occur at a significantly lower rate than direct excitations so that radiation to the ground state causes the $2\,^1P$ and $2\,^1S$ levels to deplete below their QSS value before the triplet states approach their QSS value at which exchange collisions are competitive with other processes. In this situation the overshoot of the continuum rate arises because the triplet states maintain a significant positive rate while the singlet state rates because increasingly unimportant. The subsequent rate decay to QSS follows the acquisition of QSS by the triplet states.

Those cases which appear to go monatonically to QSS (cases A and D) do so for slightly different reasons. Case A, the high-density case, is sufficiently collision dominated that, although radiation effects still determine the total rate for those low levels, collisions are sufficiently rapid to prevent oscillation and cause the ground state and continuum to converge to the QSS together. Case D, the low-temperature case, is sufficiently radiation dominated that the $2\,^1P$ radiative depopulation serves to depress the density of adjacent levels. Thus, instead of the $2\,^3S$ populating radiatively until collisional depopulation balances it, the $2\,^3S$ collisional population rate decreases rapidly enough for the collisional-radiative processes to balance each other at a lower density. Hence there is no significant increase in density and the ground-state and continuum rates converge to QSS together.

A dominant feature of the analysis of these plasmas has been the effect of the metastable level upon the time required to reach QSS. The other levels adjust to some value near or below their QSS value early in the decay, typically at times on the order of 10^{-8} sec, which is characteristic of radiative decay times. Then, as the metastable levels continue to populate radiatively, collisional processes from the metastable levels to the adjacent levels and subsequent excitation to higher levels serve to raise the densities of these levels to their final QSS values. The amount of adjustment was dictated by the energy proximity to the metastable levels and whether the collisional excitations were governed by direct or exchange calculations. The importance of these metastable levels upon the time for a plasma to achieve QSS should not be neglected.

D. Time Development of CRR Applied to Free-Electron Density

Because of the very appreciable time required for QSS to be obtained for some of the plasmas, as shown by $\dot{n}_e/\dot{n}(1)$ in Figs. 1–3, it is of interest to observe the time development of the CRR coefficient $\alpha(t)$. This is also shown in Figs. 1–3 for the plasmas studied here. The somewhat surprising thing revealed by $\alpha(t)/\alpha(\mathrm{QSS})$ compared to $\dot{n}_e/\dot{n}(1)$ is that the continuum decay can in general be described adequately by CRR theory significantly before QSS is actually obtained. For example, case C does not acquire QSS within 5% according to $\dot{n}_e/\dot{n}(1)$ until $t = 10^{-4}$ sec, whereas $\alpha(t)$ overshoots the QSS value by a maximum of 5% at $t = 1\times10^{-7}$ sec and remained within 5% thereafter. Two of the plasmas (cases B and F) for $T_e = 10\,000\,^\circ\mathrm{K}$ have $\alpha(t)$ which deviate substantially (20–25%) above the QSS value, but in light of the deviation from QSS of the $\dot{n}_e/\dot{n}(1)$ curves for these cases, this is not as serious as would have been expected. The two cases, which do not follow this pattern, cases A and E, have different characteristics. Case A, the high-density case, has an $\alpha(t)/\alpha(\mathrm{QSS})$ which converges to QSS with the same characteristics of $\dot{n}_e/\dot{n}(1)$ and in either case is quite rapid. Case E, the high-temperature case, is characterized by an almost 50% overshoot of the $\alpha(t)/\alpha(\mathrm{QSS})$ and then steady convergence back to the QSS with $\dot{n}_e/\dot{n}(1)$. This large overshoot in the $\alpha(t)/\alpha(\mathrm{QSS})$ for case E is attributed to it being more collision dominated so there is better communication between the continuum and the low-lying quantum states.

The conclusion from this, that CRR can be applied to the continuum rate for low-density ($n_0 \leq 10^{15}\ \mathrm{cm}^{-3}$) low excitation temperature ($T_e \leq 10\,000\,^\circ\mathrm{K}$) plasmas appreciably before QSS is acquired, is inescapable. The reason for this applicability of CRR to the continuum decay is fairly straightforward. If one writes the ERE equation for the rate of change of the ground state and factors out n_e^2 to put it into the proper form for identifying the CRR coefficient, one sees that the dominant contributors to the ground-state rate are those terms involving the low-lying energy levels, particularly radiation from the $2\,^1P$ level. Because of the energetically close proximity of the $2\,^1P$ level to the $2\,^3S$, $2\,^3P$, and $2\,^1S$ levels, and the significant times for them to reach their QSS value, it will require significant times for the QSS to be reached, so far as the ground state is concerned. However, for the "less collision dominated" plasmas, the upper

quantum levels are the most important so far as the transfer of electrons between the continuum and the bound states are concerned. The lower levels populate by radiation from the upper levels. Hence the continuum develops equilibrium with the upper states very rapidly and decays with them according to CRR as they radiatively fill the low levels until QSS for the entire plasma is obtained.

It should be noted that this analysis would only be valid for those plasmas in which the population density of the metastable levels is increasing. If these levels are depopulating, this must be done through excitation to some higher bound level and then subsequent ionization thus adjusting the time-dependent recombination rate to some lower value.

E. Effect on Measurements

The results presented in the preceding sections indicate that when plasma conditions are changing there may be inconsistencies in attempting to correlate experimental and theoretical results. If measurements of recombination coefficients are based upon the electron-density decay rates, the resultant values will show a tendency to be above calculated values if the QSS has not been established. If measurements of excited-state population densities are made and these values used to determine the recombination coefficients, they will have a tendency to be below the QSS values.

There has been considerable investigation of helium recombination reported in the literature but the unusually detailed nature of the present study makes it difficult to examine the experiments meaningfully. The present study requires time-dependent measurements of a large number of excited-state densities and the election density whereas to meet the goal of most experimental investigations, the electron density and only a few excited-state densities will suffice. An exception is the recent work of Johnson and Hinnov[8] in which they report simultaneous measurements of electron density and excited-state population densities as functions of time for afterglow helium plasmas. The purpose of their work was to obtain cross section functional forms so that QSS calculations and measurements would be in closer agreement. A distinct feature of their reported data is that in the very early portion of the decay when plasma parameters are changing the fastest, recombination rates from the electron density measurements are approximately a factor of 2 greater than the recombination rates based upon excited-state densities. The qualitative agreement of these data with the results of the previous sections lends support to the possibility that at those early measurement times the QSS had not yet developed. Quantitative verification will require development of an ERE solution which allows T_e to change, which will be an even more lengthy computation than the present one.

IV. CONCLUSIONS

The results and analyses presented in the preceding sections, based upon the transient solution to the ERE for a decaying helium plasma, show that in the range of conditions studied (Table I), acquisition of the QSS is not necessarily as rapid as previously supposed. For the low-electron-density plasma ($n_e = 1.5 \times 10^{12}$ cm^{-3}) studied this time was of the order of 10^{-4} sec. Times for higher electron densities were generally of the order of 10^{-8}–10^{-5} sec. The principal contributor to this relatively lenghty time is the transient coupling between the metastable $2\,^3S$ state and other bound states.

Although the QSS may require physically appreciable times to be established, the free-electron density can be described by the CRR coefficients considerably earlier in all but the high-temperature ($T_e = 14\,000\,^\circ$K) or high-density cases ($n_0 \approx 1.6 \times 10^{17}$ cm^{-3}). For the high-density cases, the time to achieve QSS is, however, generally small, $t \leq 5 \times 10^{-8}$ sec.

If measurements of electron density and excited-state densities are made simultaneously in a period before QSS is established, recombination rates based upon the excited-state densities will be spuriously low. Rates based upon the electron density will be slightly high but are more accurate than the rates based upon excited-state densities. Use of the population densities together with the electron density and the QSS assumption to determine collisional rates or cross sections between bound levels must be approached carefully to insure that QSS is valid.

There is evidence that the Gryzinski[16] formulation for the excitation cross sections are larger than the actual cross sections.[9] This will have a tendency to make results reported here conservative; the times based upon smaller cross sections would be longer.

Because of the limited lower range of plasma conditions for which the present computer program can be used, application of the results presented here to published experimental conditions must be largely qualitative. However, the features of the ERE solution illustrating the transient coupling between the metastable $2\,^3S$ state and other states provide a great deal of insight into the mechanism by which QSS is established. The study of physical plasmas in which electron temperature is constantly changing will require development of an ERE solution in which the electron temperature is continuously variable, a significantly more difficult problem.

ACKNOWLEDGMENTS

The authors gratefully acknowledge the continuing stimulating encouragement of Dr. W. K. McGregor, Jr. and the advice and assistance of F. C. Loper and E. W. Dorrell, Jr., Central Computer Operations, who suggested the numerical technique and performed the initial programming for this work.

*Research sponsored by Arnold Engineering Development Center, Air Force Systems Command, Arnold Air Force Station, Tenn. under Contract No. F40600-71-C-0002 with ARO, Inc. Further reproduction is authorized to satisfy the needs of the U.S. Government.

†Research engineer, T-Projects Branch, Engine Test Facility.

‡Associate Professor, Physics Department.

[1]D. R. Bates, A. E. Kingston, and R. W. P. McWhirter, Proc. Roy. Soc. (London) A267, 297 (1962); A270, 155 (1962).

[2]N. D'Angelo, Phys. Rev. 121, 505 (1961).

[3]S. Byron, R. C. Stabler, and P. I. Bortz, Phys. Rev. Letters 8, 376 (1962).

[4]D. R. Bates and A. E. Kingston, Proc. Phys. Soc. (London) 83, 43 (1964).

[5]E. Hinnov and J. G. Hirschberg, Phys. Rev. 125, 795 (1962).

[6]F. Robben, W. B. Kunkel, and L. Talbot, Phys. Rev. 132, 2363 (1963).

[7]C. B. Collins and W. B. Hurt, Phys. Rev. 167, 166 (1968).

[8]L. C. Johnson and E. Hinnov, Phys. Rev. 187, 143 (1969).

[9]W. A. Rogers and M. A. Biondi, Phys. Rev. 134, 1215 (1964).

[10]C. J. Chen, J. Chem. Phys. 50, 1560 (1969).

[11]R. W. P. McWhirter and A. G. Hearn, Proc. Phys. Soc. (London) 82, 641 (1963).

[12]H. W. Drawin, J. Quant. Spectry. Radiative Transfer 10, 33 (1970).

[13]C. C. Limbaugh, W. K. McGregor, and A. A. Mason, Arnold Engineering Development Center Technical Report No. AEDC-TR-69-156, 1969 (unpublished).

[14]B. F. Gordiets, L. I. Gudsenko, and L. A. Shelepsin, J. Quant. Spectry. Radiative Transfer 8, 791 (1968).

[15]D. R. Bates and A. E. Kingston, Proc. Roy. Soc. (London) A279, 10 (1964); A279, 32 (1964).

[16]M. Gryzinski, Phys. Rev. 138, 305 (1965); 138, 322 (1965); 138, 336 (1965).

[17]F. E. Niles, Ballistic Research Laboratories Report No. 1354, 1967 (unpublished).

[18]L. C. Green, R. P. Rush, and C. D. Chandler, Astrophys. J. 3, 37 (1950).

[19]C. E. Moore, *Atomic Energy Levels* (Natl. Bur. Std., U.S. GPO, Washington, D.C., 1949).

[20]M. F. Seaton, Roy. Astro. Soc. Mon. Not. 119, 81 (1959).

[21]B. Noble, *Numerical Methods: II Difference Integration and Differential Equations* (Interscience, New York, 1964), Vol. II, Chap. 10, p. 256; J. B. Scarborough, *Numerical Mathematical Analysis* (Johns Hopkins Press, Baltimore, 1966), 6th ed., Chap. 13, p. 310.

[22]H. W. Drawin, F. Emard, and H. O. Tittle, Ninth International Conference on Phenomena in Ionized Gases, Bucharest, 1969 (unpublished).

[23]M. A. Gusinow, J. B. Gerardo, and J. T. Verdeyin, Phys. Rev. 149, 91 (1966).

[24]G. K. Born and R. G. Buser, Phys. Rev. 181, 423 (1969).

PHYSICAL REVIEW A VOLUME 4, NUMBER 6 DECEMBER 1971

Scintillation of Liquid Helium under Pressure. I. $4.2 > T > 1.3$ °K*

Robert J. Manning,† Forrest J. Agee, Jr.,‡
James S. Vinson,‡§ and Frank L. Hereford
Department of Physics, University of Virginia, Charlottesville, Virginia 22901

(Received 2 August 1971)

The intensity of α-particle-produced scintillations of liquid helium has been measured in the 1.3–4.2 °K temperature range and at pressures varying from the vapor pressure at 1.3 °K to 28 atm.

I. INTRODUCTION

Among the unusual properties of superfluid liquid helium is a reduction in the intensity of the scintillation of the fluid produced by α particles as its temperature is lowered.[1] A number of investigations have been carried out, involving the effects on scintillation of an electric field,[2] a heat current,[3] and rotation of the fluid.[4]

We present here the results of measurements of the scintillation of pressurized liquid helium. An extension of the measurements to lower temperatures is described in the following paper (II)[5] and the results interpreted in the light of other recent investigations. Specifically, these involve our observations of both the scintillation *pulse* intensity and the *total* intensity of the He II luminescence,[6] with results which confirmed a suggestion made earlier by Moss and Hereford[1] that delayed emission from metastable states could be responsi-